Mechanisms of Decomposition of α-Hydroxydialkylnitrosamines in Aqueous Solution

ARTICLE *in* CHEMICAL RESEARCH IN TOXICOLOGY · NOVEMBER 2000

Impact Factor: 3.53 · DOI: 10.1021/tx000084p · Source: PubMed

4 AUTHORS, INCLUDING:

Milan Mesić
University of Osijek
46 PUBLICATIONS **260** CITATIONS
SEE PROFILE

Jari Peuralahti
PerkinElmer
12 PUBLICATIONS **189** CITATIONS
SEE PROFILE

Mechanisms of Decomposition of α-Hydroxydialkylnitrosamines in Aqueous Solution

Milan Mesic', Jari Peuralahti, Patrick Blans, and James C. Fishbein*

Department of Chemistry and Biochemistry, University of Maryland Baltimore County, 1000 Hilltop Circle, Baltimore, Maryland 21250

Received April 11, 2000

A study of the decomposition of α-hydroxydialkylnitrosamines in aqueous 9% acetonitrile, with an ionic strength of 1 M ($NaClO_4$), at 25 °C is reported. Plots of the logarithm of the buffer-independent rate constant, k_o, against pH are concave up and indicate a three-term rate law for the solvent reaction, including acid (k_{H^+})-, base (k_{OH})-, and pH-independent (k_{HOH}) terms. Secondary α-deuterium isotope effects for compound **1a**, (*N*-nitrosomethylamino)-phenylmethanol, are as follows: $k^{\alpha}_{H}/k^{\alpha}_{D} = 1.12 \pm 0.03$ and 1.19 ± 0.02 for k_{H^+} and k_{OH}, respectively. General acid (k_{HA}) and general base (k_{A^-}) catalysis by more acidic carboxylic acid buffers is also observed. Structure reactivity and other parameters obtained in this study, and their changes with substrate and catalyst structure, permit the assignment of mechanisms for the k_{H^+}, k_{OH}, k_{HA}, and k_{A^-} processes.

Introduction

α-Hydroxydialkylnitrosamines are reactive intermediates that are believed to be formed by the action of P450 enzymes on the parent dialkylnitrosamines (*1*−*3*). They decompose to form diazonium ions and in some cases carbocations that can alkylate DNA, the reaction that is believed to be responsible for the mutagenicity and carcinogenicity of dialkylnitrosamines.

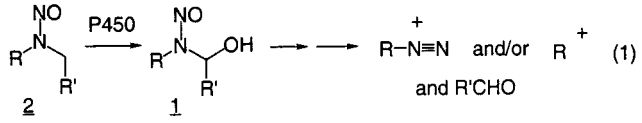

2 1 (1)

At one time, it appeared that such species might be too unstable to be characterized, but through elegant work nearly 20 years ago, a number of α-hydroxymethyl compounds **1** (R′ is H) were synthesized and their stabilities were characterized in aqueous media (*4*, *5*). Some variation in R (R can be unbranched and branched alkyl groups) indicated little change in reactivity as a function of structure. In the intervening years, two reports of highly stable α-hydroxynitrosamines have appeared (*6*, *7*). Work from this group has shown that elaboration of the R′ group in eq 1 (R′ is CH_3 or Ph, for example) engenders significant instability (*8*, *9*). Similarly, carbocyclic α-hydroxynitrosamines appear to be significantly more unstable than the α-hydroxymethyl compounds originally reported (R′ is H, above) (*10*).

With a single exception (*8*), there has been little focus on the detailed mechanisms by which α-hydroxydialkylnitrosamines decompose and the way in which these mechanisms manifest effects of structure on reactivity. Such mechanisms and structure−reactivity relations impact on the lifetimes and thus diffusibility of alkylating equivalents and, with some caveats, the possibility of targeting of alkylation events. This work summarizes experiments with the compounds below that were designed to give a detailed picture of the mechanisms of decomposition of α-hydroxydialkylnitrosamines.

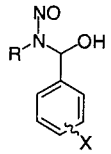

1, X = H
1a, R = -CH_3
1b, R = -$CH_2CH_2OCH_3$
1c, R = -$CH_2CH(OCH_3)_2$
1d, R = -CH_2CH_2CN

2, R = -CH_3, X= 3-Cl
3, R = -CH_3, X = 4-Cl
4, R = -CH_3, X = 4-CF_3

These compounds are generated by reduction of α-hydroperoxy precursors in acetonitrile and are studied in largely aqueous media by means of stopped-flow techniques. Previous spectroscopic, kinetic, and product analyses have demonstrated the utility of this approach to examining the chemistry of these reactive intermediates (*8*−*10*). This study has permitted the first description of the hydronium ion- and hydroxide ion-catalyzed mechanisms, the latter being dominant in the physiological pH region for the substrates that were studied. Further, the mechanisms of heretofore unknown general acid- and general base-catalyzed reactions are also deduced.

Experimental Section

Warning: *All N-nitroso compounds must be regarded as suspect carcinogens and handled appropriately using double pairs of frequently changed gloves as well as standard laboratory garments. All materials suspected of contact with such compounds were treated with 50% aqueous sulfuric acid containing the commercially available oxidant NoChromix.*

Materials. The α-hydroperoxynitrosamine precursors to α-hydroxynitrosamines were prepared by minor modification of the original procedure (*4*, *5*, *11*, *12*). This involved group exchange starting with the α-chloroacetate esters in a mixture of aqueous hydrogen peroxide and acetonitrile, followed by extraction and purification by preparative thin-layer chomatography. Synthesis of the esters was previously published (*13*). The synthesis of the α-deuterated substrate, [α-^{2}H]-**1a**, for the measurement of secondary α-deuterium kinetic isotope effects was carried out as described for the protio compound, starting with deuterated benzaldehyde that was generated by the Neff

10.1021/tx000084p CCC: $19.00
Published on Web 09/23/2000

reaction, as described previously (*14*). ^{1}H NMR indicated <3% contamination by protium in the benzaldehyde prior to synthesis of the α-hydroperoxy compound and after decomposition in D_2O as described below.

A typical synthesis for the α-hydroperoxynitrosamine precursors of α-hydroxynitrosamines is given for compound **2**. Spectral data for the other α-hydroperoxynitrosamines follow. The ^{1}H NMR spectra, samples of which are included in the Supporting Information, indicate that the purity of the α-hydroperoxynitrosamines is on the order of ≥95%, with most significant common contaminants being solvents of purification or the substituted benzaldehydes of decomposition, the latter increasing with storage time at −20 °C.

α-Hydroperoxy(3-chlorophenylmethyl)-*N*-methylnitrosamine (2). *N*-Nitroso-*N*-methyl (3-chlorophenyl)methylchloroacetate (5.1 mmol) was dissolved in 14 mL of acetonitrile. A 25 mL volume of 30% H_2O_2 was added dropwise to the mixture. Some precipitation appeared, and 10 mL of acetonitrile was added to the mixture which was then stirred overnight. The resulting mixture was clear, and 15 mL of water and 15 mL of CH_2Cl_2 were added. The product was extracted into the CH_2Cl_2 which was washed with water. The CH_2Cl_2 solution was dried with Na_2SO_4. The product was purified by preparative TLC using 20% ethyl acetate in hexane as the eluent. ^{1}H NMR ($CDCl_3$): δ 9.96 (1H, s), 7.41−7.21 (5H, m), 2.85 (3H, s). ^{13}C NMR ($CDCl_3$): δ 134.6, 134.1, 129.7, 129.6, 129.3, 125.8, 123.7, 95.1, 26.5. In certain cases, there was evidence of both *E* and *Z* rotamers, but due to overlaps and the preponderance of the *E* form, it was not always possible to ditinguish signals for all hydrogens in the *Z* forms. ^{1}H NMR for (*E*)-**3** ($CDCl_3$, *E*/*Z* ∼ 40): δ 9.47 (1H, s), 7.43−7.21 (5H, m), 2.87 (3H, s). ^{1}H NMR for (*Z*)-**3** ($CDCl_3$, *E*/*Z* ∼ 40): δ 3.72 (3H, s). ^{13}C NMR for **3** ($CDCl_3$): δ 136.1, 131.5, 129.5, 127.8, 96.0, 27.1. **4** was crystallized from pentane. ^{1}H NMR ($CDCl_3$): δ 10.17 (1H, s), 7.71 (2H, d), 7.49 (2H, d), 7.421 (1H, s), 2.87 (3H, s). ^{13}C NMR ($CDCl_3$): δ 136.1, 131.5, 129.5, 127.8, 96.0, 27.1. ^{1}H NMR for **1b** ($CDCl_3$): δ 9.63 (1H, s), 8.06 (1H, d), 7.38 (5H, m), 3.72 (2H, t), 3.56 (2H, t), 3.35 (3H, s). ^{1}H NMR for (*E*)-**1c** ($CDCl_3$, *E*/*Z* ∼ 20): δ 10.74 (1H, s), 7.42−7.32 (6H, m), 4.90 (1H, dd), 3.92 (1H, dd), 3.40 (6H, s), 3.00 (1H, dd). ^{1}H NMR for (*Z*)-**1c** ($CDCl_3$, *E*/*Z* ∼ 20): δ 3.08 (6H, s). ^{1}H NMR for (*E*)-**1d** ($CDCl_3$, *E*/*Z* ∼ 14.5): δ 9.15 (1H, s), 7.65−7.25 (6H, m), 3.86 (1H, m), 3.35 (1H, m), 2.70 (1H, m). ^{1}H NMR for (*Z*)-**1d** ($CDCl_3$, *E*/*Z* ∼ 14.5): δ 4.4 (1H, m), 4.2 (1H, m), 2.9 (1H, m). ^{13}C NMR ($CDCl_3$): δ 131.8, 129.4, 128.6, 125.4, 95.6, 36.2, 14.6.

Methods. (1) Products. Product analysis was carried out by ^{1}H NMR. The hydroperoxide in CD_3CN was reduced with 1.1 equiv of tributylphosphine. Immediately after reduction and mixing, the CD_3CN solution was rapidly mixed at room temperature with aqueous buffer. Aqueous reaction solutions were made up with D_2O containing $DClO_4$ or solutions buffered with CD_3COOD and its base form and contained *tert*-butyl alcohol as an internal standard. Control experiments with authentic aldehydes indicated that the signal intensity of the aldehydic proton was 79% of that of the CH protons of *tert*-butyl alcohol at equimolar concentrations. The aldehydic proton was used to quantitate yields, so the reported yields are normalized by a factor of 0.79 for the difference in response.

(2) Kinetics. Procedures have been previously described (*8*). Kinetics were monitored using an Applied Photophysic DX17MV stopped-flow spectrophotometer by monitoring the increase in absorbance of the aldehyde at 245, 255, or 265 nm. Reaction was initiated by mixing a 10-fold excess of aqueous buffer with 1 volume of hydroperoxide in acetonitrile that had been previously reduced by addition of 1 equiv of tributylphosphine. Reduced stock solutions of hydroperoxide were typically generated and stored at −40 °C and discarded within 1 h of the reduction.

Results

Products. The products of decomposition were investigated by ^{1}H NMR by carrying out the decomposition reactions in D_2O buffered with 0.1 M d_4-acetic acid buffers (DA/A = 1) or 0.1 M $DClO_4$ solutions. A solution of the α-hydroperoxy precursor in CD_3CN was reacted with 1.1 molar equiv of tributylphosphine, and a volume of this was reacted with a 5.6-fold excess of aqueous media. The final concentration of the nitrosamine was typically 0.01 M, and the yields were determined by comparison with the internal standard *tert*-butyl alcohol (∼0.001 M). The yields are summarized in Table 1. Inspection of the spectra indicated no signal at 2.41 ppm (for $CH_3ND_3^+$). Based on the maximum height of the noise, the upper limit for $CH_3ND_3^+$ was 5% of that for methanol.

Table 1. Summary of Products for Reactions in D_2O Solutions (15 vol % CD_3CN) Quantified by ^{1}H NMR[a]

	product (yield[b])	
compd	reaction in 0.1 M $DClO_4$	reaction in 0.1 M CD_3COOD and 50% anion
2	$CH_{3-x}D_xOD$ (83 ± 9%)	$CH_{3-x}D_xOD$ (79 ± 5%)[c]
	3-ClPhCHO (99 ± 5%)	3-ClPhCHO (105 ± 6%)[c]
3	$CH_{3-x}D_xOD$ (81 ± 9%)	$CH_{3-x}D_xOD$ (75 ± 3%)
	4-ClPhCHO (99 ± 9%)	4-ClPhCHO (106 ± 5%)
1d	$NCCH_{2-x}D_xCH_{2-y}D_y$-OD (83 ± 5%)	$NCCH_{2-x}D_xCH_{2-y}D_y$-OD (78 ± 4%)
	PhCHO (97 ± 6%)	PhCHO (95 ± 5%)

[a] Reactions at room temperature. [b] Relative to the internal standard *tert*-butyl alcohol. Unless otherwise noted, values are based on single experiments, and means and standard deviations are based on quadruplicate analysis of the single experiment. For the product alcohol from **1d**, integration of the hydroxymethylene proton was used. [c] Experiment carried out in duplicate.

An experiment with **1a** (concentration of $\sim 1 \times 10^{-4}$ M) was carried out in 0.1 M $HClO_4$ and 20 vol % CH_3OH, and the products were analyzed by HPLC. Based on the retention time and integration factor, determined by a three-point standard curve, of the authentic α-methoxy compound (*13*), an upper limit for the yield of the α-methoxy compound, which was not detected, was less than 3%.

Kinetics. (1) Solvent Reactions. For all compounds studied at all pH values, the kinetics of aldehyde product formation, monitored at 245, 255, or 265 nm, exhibited good first-order behavior for more than four half-lives of reaction. Plots of k_{obsd} against buffer concentration, containing at least three points spanning the concentration range of 0.05−0.3 M, were generally linear, maximal increases being less than 100% of the intercept value extrapolated to zero buffer concentration. Typical plots are shown in Figure 1. Included in Figure 1 are results from control experiments in which the addends trifluoroacetate ion and acetamide were varied over a similar concentration range. The intercept values of the buffer dilution plots were taken as buffer-independent rate constants, k_o. The values of log k_o for all compounds, except **1a** (*8*), that were studied are plotted against pH in Figure 2.

The solvent deuterium isotope effects on decomposition of compounds **1a**, **2**, and **3** were determined in 0.1 M $LClO_4$ (L is H or D). For these determinations, the H_2O and D_2O reactions were carried out on the same day in sequence for a given compound and the values of k_{obsd} for each compound in each solution were based on replicates of not less than 12 runs. The values of k_{H_2O}/k_{D_2O} for compounds **1a**, **2**, and **3** are 0.82, 1.15, and 1.31 (±<8%), respectively.

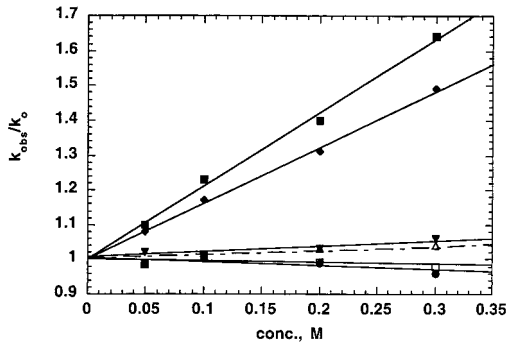

Figure 1. Plot of k_{obsd} divided by k_o, the buffer- or addend-independent rate constant, vs buffer or addend for the decay of α-hydroxynitrosamines, aqueous 9% acetonitrile, with an ionic strength of 1 M ($NaClO_4$), at 25 °C: (●) **1a**, varying acetamide at [$HClO_4$] = 0.01 M; (□) **1a**, varying sodium trifluoroacetate, [dichloroacetate buffer, 50% anion] = 0.05 M; (■) **1a**, varying methoxyacetic acid buffer, 50% anion; (◆) **4**, varying chloroacetic acid buffer, 50% anion; (▼) **1a**, varying cacodylic acid buffer, 50% anion; and (△) **1a**, varying acetate buffer, 65% anion.

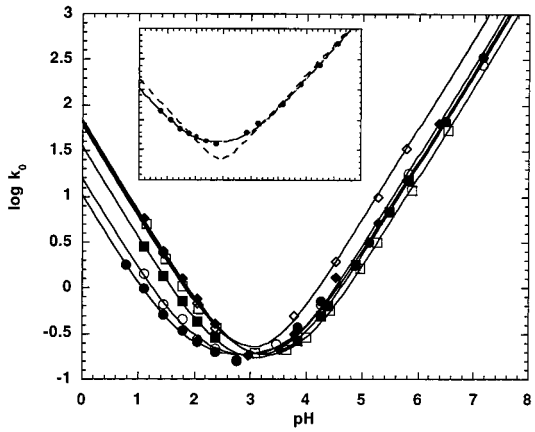

Figure 2. Plot of the log of k_o, the buffer-independent rate constant for decay of α-hydroxynitrosamines in aqueous 9% acetonitrile, with an ionic strength of 1 M ($NaClO_4$), at 25 °C, vs pH: (□) **1b**, (◆) **1c**, (◇) **1d**, (●) **4**, (○) **3**, and (■) **2**. Solid lines are fits to the equation $k_o = k_{H^+} + k_{HOH} + k_{OH}$ (see the text). The inset is the plot for **1b**, where the dashed line is the fit for $k_o = k_{H^+} + k_{OH}$ (see the text).

The secondary α-deuterium isotope effect on decomposition of **1a** was determined under two conditions at 25 °C, an ionic strength of 1 M, and 9 vol % acetonitrile. Reaction solutions contained either 0.1 M $HClO_4$ or 0.05 M acetic acid buffer, 90% base form. In the latter case, control experiments indicated for the protio compound that the value of k_{obsd} was less than 5% greater than the value of k_o, the buffer-independent rate constant. Reactions with the protio and deuterio compounds were carried out under one set of conditions on the same day in sequence, with replicate determinations of k_{obsd} for each compound being comprised of not less than 11 runs. The value of $k^{\alpha}_H/k^{\alpha}_D = 1.12 \pm 0.03$ and 1.19 ± 0.02 in 0.1 M HCl and 0.05 M acetic acid buffer (90% base form), respectively.

(2) Buffer-Catalyzed Reactions. For compounds **1a**, **1c**, and **4**, a systematic study of the effects of buffer concentration on k_{obsd} was undertaken in the pH region between pH 2 and 5. Figure 1 illustrates the fact that increasing concentrations of more acidic carboxylic acid buffers catalyzed the decay of the α-hydroxynitrosamines. The slopes of the lines in Figure 1 were taken as the catalytic constants k_{cat}, and values of k_{cat} were determined at no fewer than three different buffer ratios. Plots of k_{cat} against fraction buffer base were linear, and the intercepts of such plots at fraction base = 0 and 1 were taken as the buffer acid and base catalytic constants, k_{HA} and k_{A^-}, respectively. Values of these constants for three carboxylic acid buffers are summarized in Table 2.

Table 2. Rate Constants for General Acid and Base Catalysis of Decomposition of α-Hydroxydialkylnitrosamines at 25 °C, with an Ionic Strength of 1 M ($NaClO_4$), in 9 vol % Acetonitrile[a]

	1a (R = CH_3, X = H)	**1d** (R = CH_3, X = 4-CF_3)	**3** [R = $(CH_3O)_2$-$CHCH_2$, X = H]
CH_3OCH_2COOH			
k_{HA}' (M^{-1} s^{-1})	0.36	0.13	0.06[b]
k_{A^-} (M^{-1} s^{-1})	0.52	0.61	0.90
$ClCH_2COOH$			
k_{HA}' (M^{-1} s^{-1})	0.81	0.27	0.32
k_{A^-} (M^{-1} s^{-1})	0.18	0.31	0.25
$NCCH_2COOH$			
k_{HA}' (M^{-1} s^{-1})	1.05	0.46	0.89
k_{A^-} (M^{-1} s^{-1})	0.062	0.1	0.05[b]

[a] From the intercepts of least-squares lines of plots of k_{cat} against the fraction base form of the catalyst. Standard errors are less than ±10% except where indicated. [b] Standard errors are ±25%.

Discussion

Products. As has been reported previously (*4*, *5*, *8*, *12*), the products quantitated, and summarized in Table 1, indicate that the principle transformation in the extremes of pH studied here proceeds with cleavage of the amino nitrogen (α-hydroxy)−carbon bond to generate aldehyde and presumably the diazoate (or diazoic acid) that gives rise to electrophilic fragments, as in eq 2 (*15*−*17*). The yields of alcohol determined (Table 1) reflect lower limits due to the likely incursion of proton-for-deuterium exchange of the diazonium ion intermediates (*16*−*18*).

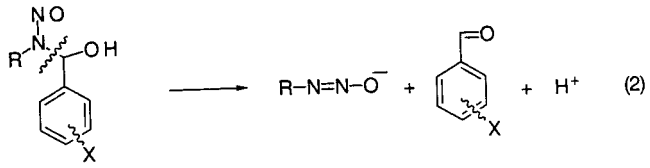

All of the product determinations reported here, with the one exception described in detail below, were carried out in deuterium oxide solutions.

Two observations rule out substantial decomposition via a nitrosiminium ion (*10*, *19*−*21*) in acidic media. Such a mechanism, below, involving initial CO bond cleavage and subsequent denitrosation of the nitrosiminium ion would yield benzaldehyde and methylammonium ion as products (*21*).

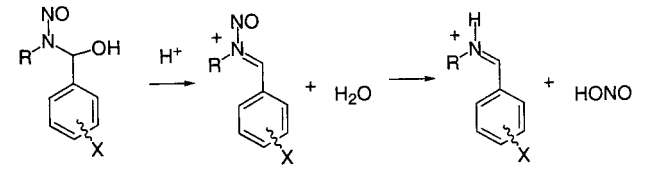

Experiments carried out in D_2O (0.1 M $DClO_4$) with NMR analysis gave an 81% yield (relative to 4-chlorobenzaldehyde) of CH_3OH and failed to detect methylammonium ion, checked by subsequent addition of the hydrochloride

salt, setting an upper limit on the yield of 5%. In a second experiment with **1a** in 20% methanolic H_2O (0.1 M $HClO_4$), HPLC analysis failed to detect the α-methoxy compound that would result from capture of a putative *N*-nitrosiminium ion by methanol. Based on the known partitioning of the cation between capture by water and by methanol (*13*), a yield of 47% is predicted assuming quantitative conversion to the nitrosiminium ion. The upper limit yield of 3% indicates that the nitrosiminium ion pathway accounts for less than 6% of the total reaction. On these bases, the contribution of a nitrosiminum ion pathway in acidic media appears to be minimal. Such a pathway has been previously proposed for decomposition of α-hydroxydialkylnitrosamines in neutral media (*22*), but there are alternative explanations for the experimental observations that gave rise to this conclusion.

Kinetics. (1) General Rate Law. In toto, the experimental evidence described in detail below requires the minimal rate law defined by eqs 3 and 4. The terms accounting for catalysis by buffer acids (k_{HA}) and bases (k_{A^-}) that were observed for some carboxylic acid buffers over a narrow pH range have been represented slightly differently in eqs 3 and 4, for reasons that will be described in detail later in the discussion. At present, it is sufficient to indicate that the mechanism of the reaction of certain carboxylic acid anions (k_{A^-}) appears to be distinct from that for the reaction of hydroxide ion (k_{OH}), while the catalysis by the proton (k_{H^+}) and some carboxylic acids (k_{HA}) is believed to be identical so that they have been summed to a single constant, k_{HA}', in eq 3. Three buffer-independent rate constants

$$k_{obsd} = k_{HA}' + k_{HOH} + k_{OH} + k_{A^-} \quad (3)$$

$$k_{HA}' = k_{H^+} + k_{HA} \quad (4)$$

for hydrogen ion-catalyzed (k_{H^+}), hydroxide ion-catalyzed (k_{OH}), and water-catalyzed (k_{HOH}) decomposition are required by the pH−rate profiles of Figure 2. This is consistent with what has been reported previously (*8*). The water-catalyzed term contributes to the overall buffer-independent term only over a narrow pH range, in contrast to simple methylene α-hydroxynitrosamines (*4*, *5*, *8*). The fact that such a reaction nonetheless contributes is indicated by the fit in the inset plot of Figure 2, which compares the best fit of the data for **3** to a three-term rate equation (solid line) and a two-term equation (dashed line) containing only terms for the hydrogen ion- and hydroxide ion-catalyzed reactions. Such fits for all compounds underestimated, by factors of 2−4, the values of k_o in the pH regions of the minima of the profiles in Figure 2. The precision of the rate constant determinations is in most cases better than ±10%, this error being too small to be consistent with the fit to the two-term rate equation. Values for the rate constants k_{H^+}, k_{HOH}, and k_{OH} derived from the best fits are summarized in Table 3. In general, the standard errors are less than ±10%, but this is not the case for most of the values of k_{HOH}, for which some of the standard errors are ±25% due to the lack of dominance of this reaction pathway.

Rate constants k_{A^-} and k_{HA} for catalysis by carboxylic acids are summarized in Table 2, and were determined as previously described (see Results).

Mechanisms. (1) k_{HA}' Reaction (eq 6). A number of pieces of experimental evidence indicate that the mechanism for catalysis by acids, both the hydronium ion and the stronger carboxylic acids (Table 2), involves concerted proton transfer and leaving group expulsion.

Table 3. Rate Constants for the Decay of α-Hydroxydialkylnitrosamines in Aqueous Solutions, at 25 °C, with an Ionic Strength of 1 M ($NaClO_4$), in 9 vol % Acetonitrile[a]

compd	R_1	X	k_H (M^{-1} s^{-1})	k_{HOH} (s^{-1})	$10^{-9}k_{OH}$ (M^{-1} s^{-1})
1a	CH_3	H	56	0.12	1.7
1b	CH_3	4-Cl	34	0.13[b]	2.1
1c	CH_3	3-Cl	16	0.14[b]	2.9
1d	CH_3	4-CF_3	10.5	0.16[b]	3.0
2	$CH_3OCH_2CH_2$	H	72	0.093[c]	3.5
3	$(CH_3O)_2CHCH_2$	H	73	0.055[c]	5.8
4	$NCCH_2CH_2$	H	24	0.084[c]	8.5

[a] Derived by nonlinear least-squares fitting with proportional weighting from the data depicted in Figure 1. Standard errors are less than ±10% except where indicated. [b] The standard error is less than ±15%. [c] The standard error is less than ±25%.

Two possible mechanisms for this concerted general acid catalysis are simple general acid catalysis, represented in eq 5, and the alternative specific acid general base catalysis, represented in eq 6.

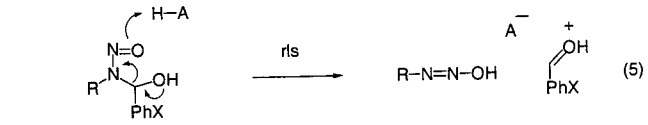

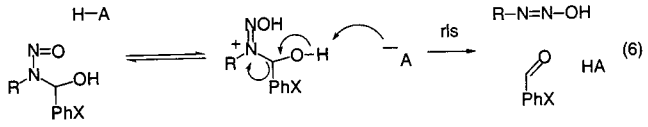

Evidence for the concerted nature of the reaction is presented in the first subsection, while the analysis that leads to the conclusion that the mechanism is as indicated in eq 6 is presented in the second subsection.

(i) Evidence for Concerted Proton Transfer and Leaving Group Expulsion. (1) The involvement of proton transfer in the rate-limiting step is indicated by the solvent deuterium isotope effect on catalysis by the hydronium ion where $k_{H^+}/k_{D^+} = 0.82-1.3$, depending on X, eq 5 or 6, when R is CH_3. This range of values is inconsistent with equilibrium protonation followed by a rate-limiting step that does not involve proton transfer (*23*). Such mechanisms, typified by the generic example of eq 7, are characterized by substantially smaller inverse solvent isotope effects k_{H^+}/k_{D^+} of 0.3−0.5 that arise from the loss of the differences in zero-point energy difference for hydrogens of the lyonium ion.

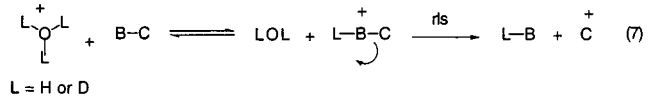

In the present case, an upper limit for such a mechanism might be as large as 0.69 (k_{H^+}/k_{D^+}) if the reaction involved equilibrium protonation of the hydroxyl oxygen, as in eq 8.

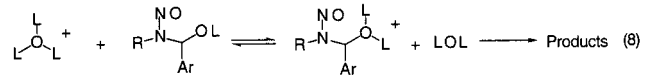

Isotope effects k_{H^+}/k_{D^+} of ~1 are typical of reactions in which the inverse isotope effect due to the disappearance of the lyonium ion is offset by a normal isotope effect that arises from the loss of zero-point energy between H and D in a transition state in which the hydrogen is "in flight" (*23*).

(2) The observation of general acid catalysis for fairly acidic carboxylic acids is also consistent with a mechanism in which a proton is transferred in the rate-limiting step (*24*, *25*). Reactions such as those in eq 7 do not exhibit catalysis by buffer acids, and the rates of such reactions are only affected by the proton concentration of the media. The observed general acid catalysis is modest; Figure 1 indicates typical rate increases at the highest buffer concentrations of less than 100%. As will be discussed below, this effect is due to both contributions of the acid as well as base form of the buffer, but the constants summarized in Table 2 indicate a significant contribution of the carboxylic acid in all cases. Despite the modest effects, control experiments (Figure 1) confirm that the increases do reflect catalysis and not medium effects. The data in Figure 1 illustrate that the addition of comparable concentrations of the very weakly basic trifluoroacetate anion and acetamide, which mimic the base and acid forms of the carboxylic acids, do not similarly increase the values of k_{obsd}. This indicates that the observed increases with cyanoacetic, chloroacetic, and methoxyacetic acid buffers are not the result of specific salt or medium effects on the reaction.

The limited structure−reactivity correlations in this study do not permit a precise determination of the position of the proton in the transition state, but are in two cases consistent with a proton in flight. The slopes of the three point Bronsted plots of log k_{HA} against pK_a for the three carboxylic acid catalysts are $\alpha = -0.38$ and -0.42 ($r^2 = 0.999$ and 0.968, respectively) for compounds **1a** and **4**. These values of α are intermediate between normally limiting values of 0 and −1 that are observed for mechanisms of catalysis in which the rate-limiting step involves diffusional encounter/separation or assistance through hydrogen bonding (*25*); this leads to the conclusion that in the present case, the proton is in flight. The α value of −0.98 for compound **1d** ($r^2 = 0.989$) suggests that the addition of electron-withdrawing groups to the leaving group results in a change to a transition state that is highly asymmetric (product-like with respect to proton transfer). The nature and implication of this change will be described in detail in the further discussion.

(3) The secondary α-deuterium kinetic isotope effect $k_{H^+}{}^{\alpha-H}/k_{H^+}{}^{\alpha-D}$ of 1.12, determined in 0.1 M $HClO_4$, requires that there is significant rehybridization at the α-hydroxy carbon in the transition state compared to the ground state, indicative of leaving group departure and the onset of sp^2 hybridization that typifies the product aldehyde. The maximum effect, for a transition state with essentially complete N−C bond cleavage, would be expected to be 1.3−1.4, based on a number of equilibrium isotope effects determined for reactions at the carbonyl group of benzaldehyde (*26*−*28*) generally indicated in eq 9.

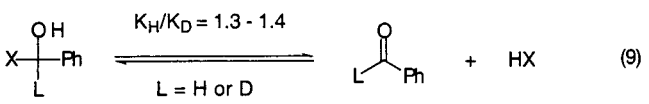

(9)

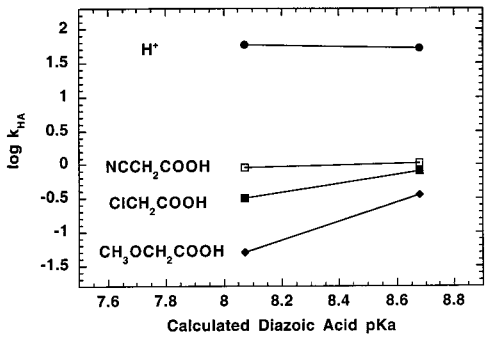

Figure 3. Plot of the logarithm of k_{HA}, the second-order rate constant for catalysis by the indicated acids, vs the pK_a calculated (17) for the diazoic acid leaving groups for compounds **1a** (pK_a = 8.68) and **1c** (pK_a = 8.07).

The observed effect on the rate constant for the present reaction suggests that the bond to the leaving diazoate anion is 40−30% [=(0.12/0.3−0.4) × 100] cleaved.

(ii) Analysis Indicating the Mechanism of eq 6 for k_{HA}'. The mechanisms of eqs 5 and 6 are an example of kinetic ambiguity, and it is not possible on the basis of the values of structure−reactivity correlations to distinguish between them. For example, both mechanisms are consistent with the positive charge buildup on the leaving group that is indicated by the positive slopes of the dependence of the logarithm of the catalytic coefficients for carboxylic acid catalysts upon the calculated leaving group pK_a (*17*) that is observed in Figure 3. A distinction is however possible because the two mechanisms make opposite predictions regarding the changes in such correlations with catalyst pK_a that are predicted by these two mechanisms (*29*−*31*). Figure 3 shows that the slopes of the lines decrease as the acid catalyst strength increases on going from methoxyacetic acid to the hydronium ion.

The changes that are predicted by the two mechanisms can be understood by examination of the three-dimensional reaction coordinate diagrams in Figure 4A for the mechanism of eq 6 and Figure 4B for the mechanism of eq 5. The "unseen" third dimension is a free energy axis that is orthogonal to the axes in Figure 4 that indicate progress along a coordinate for proton transfer and leaving group departure, respectively. As mentioned earlier, extensive structure−reactivity correlations are not available to precisely place the transition state on the map for either mechanism. However, the important point for the present purposes is that the discussion in the previous subsection establishes that the transition states for some of the reactants that have been studied are oriented diagonally with respect to the two axes for bonding changes, indicating a coupled concerted mechanism.

There is a detectable change in transition state structure that is consistent with the changes expected from the reaction coordinate diagram in Figure 4A drawn for the mechanism of eq 6 (*31*). The change in transition state structure is indicated in Figure 3 which illustrates a change in sensitivity to the diazoic acid leaving group pK_a of the second-order rate constants for catalysis by the hydronium ion and carboxylic acids. This is a change in the parameter known as β_{lg}, the magnitude of which corresponds to the slopes of the lines in Figure 3. The sensitivity to leaving group increases, with decreasing acid strength, from H_3O^+ (top) to methoxyacetic acid

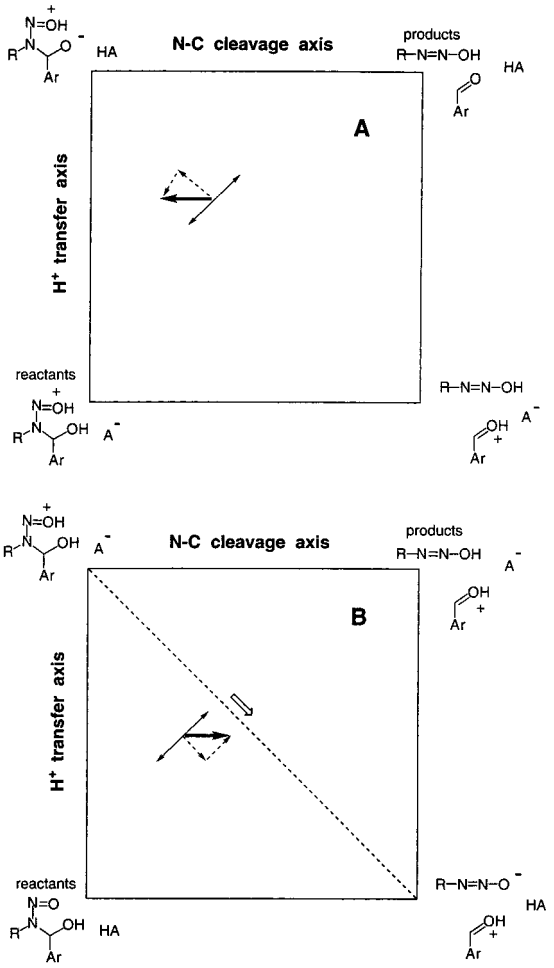

Figure 4. Reaction coordinate diagrams for the two concerted general acid-catalyzed reactions of eq 6 (A) and eq 5 (B). The orientation of the reaction path at the transition state is indicated by the double-headed arrows. The perturbations of the parallel and perpendicular components of the reaction coordinate at the transition state that result from decreasing acid strength are indicated by the dashed arrows. The resultant movement predicted for the transition state is indicated by the bold arrow.

(bottom). A positive value of the slope indicates that the more basic leaving group is more reactive and, for the least acidic catalysts, in fact bears some positive charge in the rate-limiting step. This observation requires that in the transition state for the reactions of the least acidic catalysts, proton transfer to the leaving group is more advanced than nitrogen−carbon bond cleavage. With increasing catalyst acidity, there is increasing balance between the two processes. With the hydronium ion, the near-zero slope of the line indicates little or no charge on the leaving group; proton transfer and C−N bond cleavage are more nearly balanced.

This type of change is exactly what is predicted by the reaction coordinate diagram of Figure 4A (*31*). The change from H_3O^+, a stronger acid catalyst, to methoxyacetic acid, a weaker acid, raises the lower edge of the diagram in Figure 4A relative to the upper edge. The response of the transition state to this perturbation will be to move downhill on the perpendicular axis of the reaction coordinate at the transition state and uphill along the parallel axis, as indicated by the dashed arrows in Figure 4A. The net movement is indicated by the heavy arrow in the Figure 4A. The movement, with decreasing catalyst acidity, is toward the left axis, where the leaving group has a full positive charge, and away from the right axis where the leaving group has no charge. This predicted increase in positive charge on the leaving group in changing from the catalyst H_3O^+ to methoxyacetic acid is what is indicated by the experimental data in Figure 3.

The change in transition state structure evident in Figure 3 is the opposite of that expected for a transition state for the mechanism of eq 5 that has a diagonal orientation, as indicated by the double-headed arrow in Figure 4B. The change from a stronger to a weaker acid catalyst lowers the bottom edge of the diagram in Figure 4B relative to the upper edge. The corresponding movement parallel and perpendicular to the reaction coordinate is indicated by the dashed arrows. The net movement is indicated by the bold arrow in the diagram. The projection of this movement onto the diagonal axis (open arrow) indicated by the dashed line, along which diagonal the charge on the leaving group varies from +1 (upper left corner) to −1 (lower right corner), shows that a decrease in positive charge on the leaving group is predicted with decreasing acid strength, the opposite of what is observed experimentally and illustrated in Figure 3.

(2) k_{A^-} Reaction (eq 10). It is shown below that the observed changes in structure−reactivity correlations for these rate constants can only be accommodated by a concerted transition state for the mechanism of eq 10, the specific base or general acid variant of the observed general base catalysis.

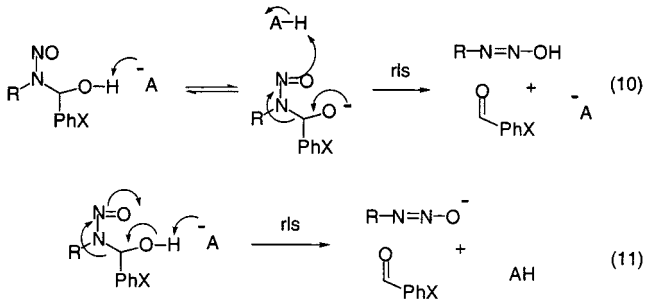

It is further concluded below that the alternative concerted general base catalysis mechanism of eq 11 is inconsistent with the observed changes.

Three types of changes in structure−reactivity relationships, which indicate changes in transition state structure, are observed in the general base-catalyzed reaction.

Figure 5 indicates (a) that the values of β_{lg}, the dependence of the catalytic constants k_{A^-} against the calculated pK_a values of the conjugate acids of the diazoate leaving groups for compounds **1a** and **1c**, change with catalyst basicity. The value of β_{lg} is slightly positive for cyanoacetate (β_{lg} = 0.15) but changes to negative values for chloroacetate and methoxyacetate (β_{lg} = −0.25 and −0.46, respectively). The slightly positive value for cyanoacetate is most consistent with the mechanism of eq 10, in which H^+ donation in the second step is slightly ahead of N−C bond cleavage. This imbalance would lead to a net positive charge development on the leaving group. The negative values in the cases of the other catalysts indicate a change in transition state structure to one in which there is negative charge buildup on the leaving group in the transition state.

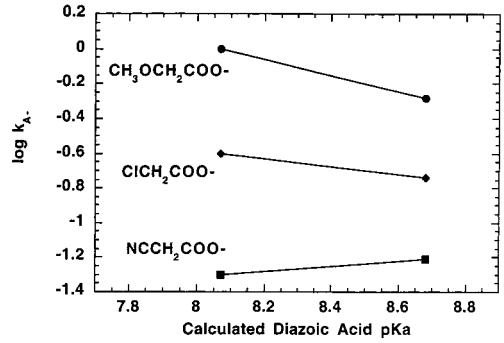

Figure 5. Plot of the logarithm of k_{A^-}, the second-order rate constant for catalysis by the indicated bases, vs the pK_a calculated (17) for the diazoic acid leaving groups for compounds **1a** (pK_a = 8.68) and **1c** (pK_a = 8.07).

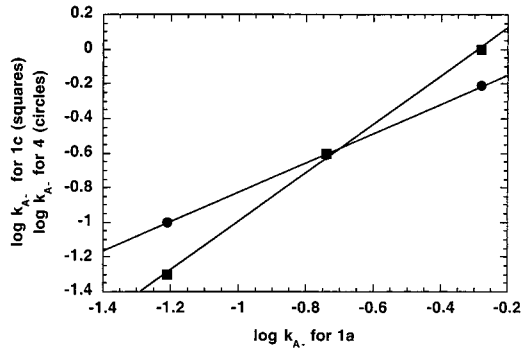

Figure 6. Plot of the logarithm of k_{A^-} for **1c** (■) and **4** (●) vs those for **1a**. The slopes of the lines are 1.4 (■) and 0.85 (●).

Additionally, there is (b) an increase in the parameter Bronsted β with increasing leaving ability of the leaving group and (c) a decrease in Bronsted β with introduction of an electron-withdrawing group in the benzene ring. The values of Bronsted β, reflecting to some degree the change in charge experienced by substituents in the catalyst due to proton transfer in the transition state, are large to intermediate with $\beta = 0.7$ ($r^2 = 0.925$), 0.57 ($r^2 = 0.904$), and 0.96 ($r^2 = 0.942$) for **1a**, **4**, and **1c**, respectively. The value near 1 for compound **1c** indicates that there is nearly unit negative charge buildup on going from the ground to the transition state, indicating the proton is almost completely transferred. The intermediate values for the other compounds suggest that the proton transfer is less complete. There is imprecision in these determinations, largely due to the systematic scatter that is sometimes observed even in a "homogeneous" series such as substituted acetic acids (*32*). The systematic nature of the scatter is indicated by the plots in Figure 6 in which the log values of the rate constants for **1c** and **4** are plotted against those for compound **1a** and show appreciably better correlations ($r^2 = 0.999$ and 0.998, respectively). They indicate that (1) there is an increase in Bronsted β with an increase in leaving group ability, changing from **1a** to **1c** [the slope (■) = 1.4], and (2) there is a decrease in Bronsted β with the introduction of an electron-withdrawing group in the phenyl ring, changing from **1a** to **4** [the slope (●) = 0.85].

The changes in structure−reactivity correlations depicted in Figures 5 and 6 are consistent with the concerted mechanism of eq 10. This can be understood with reference to the three-dimensional reaction coordinate diagram of Figure 7 in which progress with respect to proton transfer and leaving group departure in the

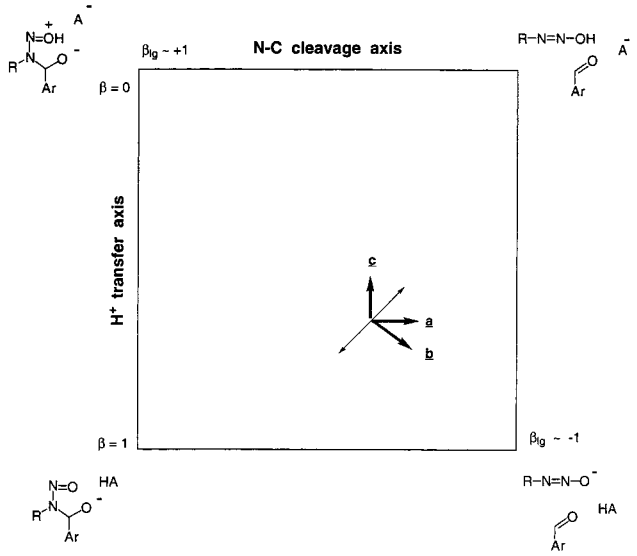

Figure 7. Reaction coordinate diagram for the proposed concerted general base-catalyzed mechanism of eq 10. The orientation of the reaction path at the transition state is indicated by the double-headed arrow. The bold arrows indicate the expected movement of the transiton state for (a) an increase in the strength of the base catalyst, (b) an increase in leaving group ability, and (c) introduction of electron-withdrawing groups into the benzene ring of compound **1a** (see the text).

rate-limiting step is measured along the two axes. The extent of charge development on the leaving group varies along the diagonal from the upper left corner (ca. +1) to the lower right corner (ca. −1). The transition state for reaction of compound **1a** is located in the lower right quadrant, consistent with a β_{lg} of ca. −0.25 (for chloroacetate) and the extent of proton transfer indicated by a Bronsted β of 0.7 and the relationship for specific base or general acid catalysis, α(for proton donation) = 1 − β(observed). The double-headed arrow indicates the orientation of the reaction coordinate at the transition state. The movements of the transition state in response to changes in catalyst strength (a, above), improved leaving group ability (b, above), and introduction of an electron-withdrawing group (c, above) are indicated by the bold arrows in Figure 7, labeled with the corresponding letters a−c, respectively. The movements are consistent with the observed effects as indicated below.

Change a. The change from the weaker catalyst chloroacetate to the more basic methoxyacetate raises the energy of the upper edge relative to the lower edge of the diagram in Figure 7. The transition state will slide downhill along the axis perpendicular to the reaction coordinate and uphill (Hammond effect) on the axis parallel to the reaction coordinate with the net movement indicated by vector **a** in Figure 7. This movement, projected onto the diagonal (from the upper left to the lower right), that indicates charge status of the leaving group predicts movement toward the lower right corner and a consequent increase in negative charge buildup on the leaving group. The increase in negative charge on the leaving group as the catalyst is changed from chloroacetate to methoxyacetate is consistent with what is observed in Figure 5, an increase in the negative slope in Figure 5 on changing from chloroacetate to methoxyacetate.

Change b. Increase in leaving group ability, changing from **1a** to **1c**, lowers the lower right corner relative to

the upper left, the two corners at which the leaving group has opposite charges. The resultant transition state movement is as indicated by the bold arrow labeled b. This movement, projected onto the vertical axis, predicts a decrease in the extent of proton donation, which is what is measured along the vertical axis. The net result is an increase in Bronsted β, consistent with the slope of >1 for the squares in Figure 6.

Change c. Introduction of an electron-withdrawing CF_3^- group into the benzene ring in compound **1a** (changing from compound **1a** to **4**) raises the energy of the right side of the diagram, relative to the left. This is because the carbonyl group is electron deficient relative to the tetrahedral carbon atom on the left edge of Figure 7. The resultant transition state movement is indicated by the bold arrow labeled c. The net movement relative to the (vertical) proton transfer axis is an increase in the extent of proton donation for **1a** compared to **4**. The net result is a decrease in Bronsted β, consistent with the slope of <1 for the circles in Figure 6.

In contrast to the above discussion, the appropriate energy surface containing a transition state with an appreciable diagonal orientation at the transition state for the mechanism of eq 11 predicts transition state movements in response to the above perturbations that are opposite to what is observed, in all cases.

(3) k_{OH} Reaction (Mechanism of eq 12). With one exception, the hydroxide ion-catalyzed reaction likely involves rate-limiting leaving group expulsion from the anionic conjugate base of the α-hydroxynitrosamine, as in eq 12 (*8*).

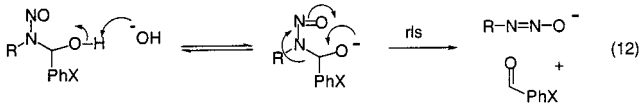

(12)

The large secondary α-deuterium kinetic isotope effect ($k_{OH}^{\alpha-H}/k_{OH}^{\alpha-D} = 1.19$) indicates a significant degree of sp^3-sp^2 rehybridization at the central carbon, consistent with leaving group bond cleavage in the transition state, as discussed above for the hydronium ion-catalyzed reaction. A plot of log k_{OH} against the calculated conjugate acid pK_a of the diazoate leaving group (not shown) has a slope of −0.88 ($r^2 = 0.98$), again suggesting that there is a significant amount of negative charge buildup on the leaving group in the transition state. Neither of these observations is consistent with rate-limiting proton transfer with hydroxide ion, the anionic intermediate which then forms products more rapidly than it reverts to reactants. The rate-limiting step for such a reaction would involve diffusion-limited encounter of hydroxide ion with the α-hydroxynitrosamine (*33*), with no rehybridization at the central carbon or significant charge buildup on the leaving group.

There is no evidence for a reaction mechanism for hydroxide ion (k_{OH}) analogous to the mechanism of eq 10, which is observed for the less basic carboxylate bases (k_{A^-}), and such a mechanism is not expected. The absence of catalysis by more strongly basic catalysts such as acetate and cacodylate anions (Figure 1) argues against the mechanism of eq 10 (and also eq 11) for the more basic hydroxide ion. The disappearance, with increasing catalyst basicity, of catalysis by the mechanism of eq 10 is expected because the driving force for catalysis decreases with increasing catalyst basicity. As formulated by Jencks (*25*, *34*, *35*), the driving force for concerted catalysis in the second step of the mechanism of eq 10 derives from the change from a thermodynamically unfavorable protonation of the nitroso oxygen in the α-hydroxynitrosamine anion in the reactants to a thermodynamically favorable protonation of the diazoate leaving group in the products. A significant driving force is required to pay for the entropically unfavorable association and proper orientation in the concerted transition state.

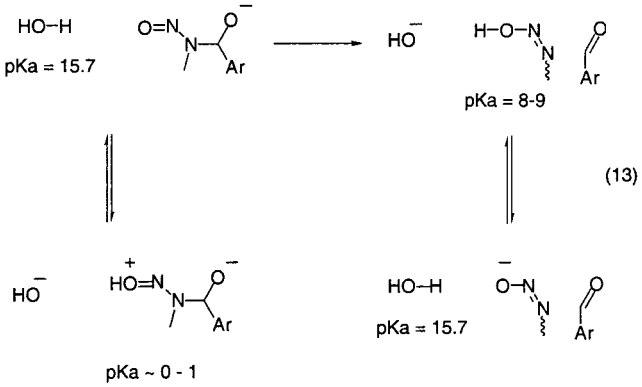

(13)

This driving force disappears as the proton transfer from the conjugate acid to the diazoate leaving group (conjugate acid pK_a ∼ 8−9) becomes less thermodynamically favorable. The absence of driving force in the case of the hydroxide ion reaction is illustrated in eq 13 in which the rate-limiting step from eq 10 (horizontal reaction) is accompanied by analysis of the thermodynamics of the relevant proton transfers in the reactants and products (vertical equilibria) (*17*, *36*). In both reactants and products, comparison of the pK_a values indicates thermodynamically unfavorable proton transfers. The absence of thermodynamic driving force makes the concerted pathway entropically disfavored, so the lowest-energy pathway is the mechanism of eq 12.

With the best leaving group studied here, compound **1d**, a change in the rate-limiting step is likely occurring. The second-order rate constant for the hydroxide ion-catalyzed reaction of compound **1d** is $\sim 9 \times 10^9$ M^{-1} s^{-1}, which approaches the value expected for a diffusion-limited proton transfer involving hydroxide of $\sim 2 \times 10^{10}$ M^{-1} s^{-1}. This indicates that the barrier for leaving group expulsion from the conjugate base of the α-hydroxynitrosamine is quite small; slightly less than half of all diffusional encounters with hydroxide ion result in product formation. Thus, both proton transfer and leaving group expulsion are partly rate-limiting in this case. It is likely that with better leaving groups, the rate-limiting step would be simple proton transfer and might well be accompanied by general base catalysis (*34*, *35*), according to the mechanism of eq 11, in which the rate-limiting step for proton abstraction by bases weaker than the anion of the α-hydroxynitrosamine would be either rate-limiting diffusional separation of the catalyst conjugate acid from the α-hydroxynitrosamine anion or, more likely, leaving group expulsion in the conjugate acid−base encounter complex.

(4) k_{HOH} Reaction. Due to the fact that this reaction is never dominant and the rate constants could only be determined with limited accuracy, the mechanism of this reaction remains the subject of ongoing inquiry.

General Implications. (1) For most α-hydroxynitrosamines studied by this group to date, the dominant mechanism at neutral pH is that of eq 12, involving equilibrium deprotonation to form the oxyanion and rate-limiting expulsion of the diazoate anion (this work and refs *8*−*10*). The rate constant for this latter process correlates quite strongly with the conjugate acid pK_a of the diazoate ($\beta_{lg} = -0.88$). The ultimate electrophilic species arising from this process is the diazonium ion. Alternative electrophilic species such as the *N*-nitrosiminium ion, and nitrosonium ion equivalents that might arise from it, are not encountered in this dominant reaction mode or any of the other mechanisms delineated in the study presented here. There is some evidence that α-hydroxynitrosamines of differing structure may in fact decompose by other modes in which alternative electrophilic species may be encountered (*6*, *7*). Both hydroxynitrosoindoles and purported α-hydroxynitrosomorpholine exhibit surprising stability compared to the compounds that we have studied here and in other reports, and exhibit products of decomposition that are not consistent with any reaction pathways elucidated in this report.

(2) This report indicates that general acid and base moieties can catalyze the decomposition of α-hydroxynitrosamines and thus establishes a chemical precedent for the involvement of biomolecules in their decay. This, combined with a further consideration, presents a possible chemical origin for the well-known "hot spots" in the mutation spectra of nitrosamine alkylating agents (*37*). The work of Gold has established that nitrosoureas covalently appended to various DNA binding agents "deliver" alkylating equivalents at the preferred sites of binding (*38*−*41*). This is surprising in light of the fact that the diazoic acids and primary diazonium ion intermediates that are involved are relatively long-lived intermediates, at least relative to diffusion in bulk solution (*42*). The observation requires that these intermediates be to some degree confined to the site of delivery. To the extent that DNA sequence contexts can activate, by exposure or by changes in pK_a, the acid and base properties of DNA bases or the phosphate backbone, the observations of acid and base catalysis in this report suggest that such sites might stimulate α-hydroxynitrosamine decomposition and subsequently be sites of enhanced alkylation. The numerous other chemical and biological factors that likely contribute to the appearance of hot spots have been discussed (*37*).

Summary

The mechanism of hydronium ion- and general acid-catalyzed decay (k_{HA}', eqs 3 and 4) of the α-hydroxydialkylnitrosamines in the study presented here is as in eq 6. Secondary α-deuterium kinetic isotope effects ($k_{H^+}^{\alpha-H}/k_{H^+}^{\alpha-D} = 1.12$), solvent deuterium isotope effecets on the k_{H^+} reaction, and general acid catalysis support a concerted mechanism. The mechanism of eq 6 is indicated by changes in structure−reactivity correlations which dictate the nature of the transition state for this reaction.

The mechanism of general base catalysis (k_{A^-}, eq 3) is as indicated in the mechanism of eq 10. This is indicated again by changes in structure−reactivity correlations.

In most cases, the mechanism of the hydroxide ion-catalyzed reaction (k_{OH}, eq 3) involves rate-limiting leaving group expulsion of the diazoate from the conjugate base of the α-hydroxydialkylnitrosamines as in eq 12. A significant amount of cleavage of the carbon-leaving group bond cleavage in the rate-limiting step is indicated by the secondary α-deuterium kinetic isotope effect ($k_{OH}^{\alpha-H}/k_{OH}^{\alpha-D} = 1.19$) and the large value of β_{lg} (−0.88).

Acknowledgment. This work was supported by Grants RO1 CA52881 and KO4 CA62124 from the National Institutes of Health.

Supporting Information Available: ^{1}H NMR spectra of **1d**, **2**, and **3** and ^{13}C NMR spectra of **2** and **3**. This material is available free of charge via the Internet at http://pubs.acs.org.

References

(1) Lawley, P. D. (1984) Carcinogenesis by Alkylating Agents. In *Chemical Carcinogens, Vol. 1* (Searle, C. E., Ed.) Vol. 182, pp 325−484, American Chemical Society, Washington, DC.
(2) Loeppky, R. N., and Michejda, C. J. (1994) *Nitrosamines and Related N-Nitroso Compounds*, American Chemical Society, Washington, DC.
(3) Lijinsky, W. (1992) *Chemistry and biology of N-nitroso compounds*, Cambridge University Press, Cambridge, U.K.
(4) Mochizuki, M., Anjo, T., and Okada, M. (1980) Isolation and Characterisation of N-Alkyl-N-(hydroxymethyl)nitrosamines from N-Alkyl-N-(hydroperoxymethyl)nitrosamines by Deoxygenation. *Tetrahedron Lett.* **21**, 3693−3696.
(5) Mochizuki, M., Anjo, T., Takeda, K., Suzuki, E., Sekiguchi, N., Huang, G. F., and Okada, M. (1980) Chemistry and Mutagenicity of α-Hydroxy Nitrosamines. *IARC Sci. Publ.* **41**, 553−559.
(6) Jarman, M., and Manson, D. (1986) The metabolism of *N*-nitrosomorpholine by rat liver microsomes and its oxidation by the Fenton system. *Carcinogenesis* **7**, 559−565.
(7) Buchi, G., Lee, G. C. M., Yang, D., and Tannenbaum, S. R. (1986) Direct acting, highly mutagenic, α-hydroxy nitrosamines from 4-chloroindoles. *J. Am. Chem. Soc.* **108**, 4115−4119.
(8) Mesic', M., Revis, C., and Fishbein, J. C. (1996) Effects of Structure on the Reactivity of α-Hydroxydialkylnitrosamines in Aqueous Solutions. *J. Am. Chem. Soc.* **118**, 7412−7413.
(9) Chahoua, L., Mesic', M., Revis, C., and Fishbein, J. C. (1997) Evidence for the formation of α-hydroxydialkylnitrosamines in the pH-independent solvolysis of α-acetoxydialkylnitrosamines. *J. Org. Chem.* **62**, 2500−2504.
(10) Chahoua, L., Cai, H., and Fishbein, J. C. (1999) Cyclic α-acetoxynitrosamines: Mechanisms of decomposition and stability of α-hydroxynitrosamine and nitrosiminium ion reactive intermediates. *J. Am. Chem. Soc.* **121**, 5161−5169.
(11) Mochizuki, M., Anjo, T., and Wakabayashi, Y. (1980) Formation of N-Alkyl-N-(1-hydroperoxyalkyl)nitrosamines from N-Alkyl-N-(1-acetoxy)nitrosamines. *Tetrahedron Lett.* **21**, 1761−1764.
(12) Okada, M., Mochizuki, M., Anjo, T., Sone, T., Wakabayashi, Y., and Suzuki, E. (1980) Formation, deoxygenation and mutagenicity of α-hydroperoxydialkylnitrosamines. *IARC Sci. Publ.* **31**, 71−82.
(13) Chahoua, L., Vigroux, A., Chiang, Y., and Fishbein, J. C. (1999) Formation and nucleophilic capture of N-nitrosiminium ions. *Can. J. Chem.* **77**, 1148−1161.
(14) Cai, H., and Fishbein, J. C. (1997) Secondary α-Deuterium Kinetic Isotope Effects in the Decomposition of Simple α-Acetoxydialkylnitrosamines: Nitrosiminium Ion Intermediates. *Tetrahedron* **53**, 10671−10676.
(15) Hovinen, J., and Fishbein, J. C. (1992) Rate Constants for the Decomposition of a Simple Alkanediazoate at Physiological pH. *J. Am. Chem. Soc.* **114**, 366−367.
(16) Hovinen, J., Finneman, J. I., Satapathy, S. N., Ho, J., and Fishbein, J. C. (1992) Mechanisms of Decomposition of (*E*)-Methanediazoate in Aqueous Solutions. *J. Am. Chem. Soc.* **114**, 10322−10328.
(17) Ho, J., and Fishbein, J. C. (1994) Rate-Limiting Formation of Diazonium Ions in Aqueous Decomposition of Primary Alkanediazoates. *J. Am. Chem. Soc.* **116**, 6611−6621.
(18) Smith, R. H., Jr., Koepke, S. R., Tondeur, Y., Denlinger, C. L., and Michejda, C. J. (1985) The Methyldiazonium Ion in Water: Competition Between Hydrolysis and Proton Exchange. *J. Chem. Soc., Chem. Commun.*, 936−937.
(19) Revis, C. L., Rajamaki, M., and Fishbein, J. C. (1995) Reexamination of the Mechanisms of Decomposition of Simple α-Acetoxynitrosamines in the Physiological pH Range. *J. Org. Chem.* **60**, 7733−7738.
(20) Cai, H., and Fishbein, J. C. (1999) α-(Acyloxy)dialkylnitrosamines: Effects of Structure on the Formation of N-Nitros-

iminium Ions and a Predicted Change in Mechanism. *J. Am. Chem. Soc.* **121**, 1826−1833.
(21) Rajamaki, M., Vigroux, A., Chahoua, L., and Fishbein, J. C. (1995) N-Nitrosiminium Ions are Ambident Electrophiles. *J. Org. Chem.* **60**, 2324−2325.
(22) Frank, N., and Wiessler, M. (1986) N-Nitroso-hydroxyalkylamine phosphate esters: a new class of N-nitroso compounds. *Carcinogenesis* **7**, 365−369.
(23) Schowen, R. L. (1972) Mechanistic deductions from solvent isotope effects. *Prog. Phys. Org. Chem.* **9**, 275−330.
(24) Jencks, W. P. (1969) *Catalysis in chemistry and enzymology*, McGraw-Hill, New York.
(25) Jencks, W. P. (1976) Enforced general acid−base catalysis of complex reactions and its limitations. *Acc. Chem. Res.* **9**, 425−432.
(26) Amaral, L. d., Bull, H. G., and Cordes, E. H. (1972) Secondary deuterium isotope effects for carbonyl addition reactions. *J. Am. Chem. Soc.* **94**, 7579−7580.
(27) Amaral, L. d., Bastos, M. P., Bull, H. G., and Cordes, E. H. (1973) Secondary deuterium isotope effects for addition of nitrogen nucleophiles to substituted benzaldehydes. *J. Am. Chem. Soc.* **95**, 7369−7374.
(28) Young, P. R., and McMahon, P. E. (1979) Separation of polar and resonance substituent effects in the reaction of benzaldehydes with HCN. A correlation cetween ρ^{r}/ρ^{r}_{eq} ratios and central atom rehybridization. *J. Am. Chem. Soc.* **101**, 4678−4681.
(29) Funderburk, L. H., Aldwin, L., and Jencks, W. P. (1978) The mechanisms of general acid and base catalysis of the reactions of water and alcohols with formaldehyde. *J. Am. Chem. Soc.* **100**, 5444−5459.
(30) Sorensen, P. E., and Jencks, W. P. (1987) The acid- and base-catalyzed decomposition of acetaldehyde hydrate and hemiacetals in aqueous solution. *J. Am. Chem. Soc.* **109**, 4675−4690.
(31) Jencks, W. P. (1985) A primer for the Bema Hapothle. An empirical approach to the characterisation of changing transition-state structures. *Chem. Rev.* **85**, 511−527.
(32) Kresge, A. J., Chen, H. L., Chiang, Y., Murrill, E., Payne, M. A., and Sagatys, D. S. (1971) Vinyl Ether Hydrolysis. III. Some Bronsted Relations and Transition State Structure. *J. Am. Chem. Soc.* **93**, 413−423.
(33) Eigen, M. (1964) Proton transfer, acid−base catalysis, and enzymatic hydrolysis. *Angew. Chem., Int. Ed.* **3**, 1−72.
(34) Jencks, W. P. (1972) General acid−base catalysis of complex reactions in water. *Chem. Rev.* **72**, 705−718.
(35) Jencks, W. P. (1972) Requirements for general acid−base catalysis of complex reactions. *J. Am. Chem. Soc.* **94**, 4731−4732.
(36) Layne, W. S., Jaffe, H. F., and Zimmer, H. (1963) Basicity of N-Nitrosamines. II. Aqueous Sulfuric Acid Solutions. *J. Am. Chem. Soc.* **85**, 1816−1820.
(37) Horsfall, M. J., Gordon, A. J., Burns, P. A., Zielenska, M., and Glickman, B. W. (1990) Mutational Specificity by Alkylating Agents and the Influence of DNA Repair. *Environ. Mol. Mutag.* **15**, 107−122.
(38) Konakahara, T., Wurdeman, R. L., and Gold, B. (1988) Synthesis of *N*-methyl-*N*-nitrosourea linked to a methidium chloride analogue and its reactions with ^{32}P-end-labeled DNA. *Biochemistry* **27**, 8606−8613.
(39) Church, K. M., Wurdeman, R. L., Zhang, Y., Chen, F. X., and Gold, B. (1990) N-(2-Chloroethyl)-N-nitrosoureas covalently bound to nonionic and monocationic lexitropsin dipeptides. Synthesis, DNA affinity binding characteristics, and reactions with ^{32}P-end-labeled DNA. *Biochemistry* **29**, 6827−6838.
(40) Mehta, P., Church, K., Williams, J., Chen, F. X., Encell, L., Shuker, D. E., and Gold, B. (1996) The design of agents to control DNA methylation adducts. Enhanced major groove methylation of DNA by an *N*-methyl-*N*-nitrosourea functionalized phenyl neutral red intercalator. *Chem. Res. Toxicol.* **9**, 939−948.
(41) Inga, A., Chen, F. X., Monti, P., Aprile, A., Campomenosi, P., Menichini, P., Ottaggio, L., Viaggi, S., Abbondandolo, A., Gold, B., and Fronza, G. (1999) N-(2-Chlorethyl)-N-nitrosourea tethered to lexitropsin induces minor groove lesions at the p53 cDNA that are more cytotoxic than mutagenic. *Cancer Res.* **59**, 689−695.
(42) Finneman, J. I., and Fishbein, J. C. (1995) Mechanism of Benzyl Transfer in the Decay of (*E*)-Arylmethanediazoates and Aryldiazomethanes in Aqueous Solutions. *J. Am. Chem. Soc.* **117**, 4228−4239.

TX000084P